Molecular Therapy
Oncolytics
Original Article

Deletion of immunomodulatory genes as a novel approach to oncolytic vaccinia virus development

Tiffany Y. Ho,[1] David Mealiea,[1,2,4] Lili Okamoto,[1,4] David F. Stojdl,[3] and J. Andrea McCart[1,2,4]

[1]Toronto General Hospital Research Institute, University Health Network, 280 Elizabeth Street, Toronto, ON M5G 2C4, Canada; [2]Department of Surgery, University of Toronto, Stewart Building, 149 College Street, Toronto, ON M5T 1P5, Canada; [3]Department of Biology, Microbiology, and Immunology, Children's Hospital of Eastern Ontario (CHEO) Research Institute, 401 Smyth Road, Ottawa ON K1H 5B2, Canada

Vaccinia virus (VV) has emerged as a promising platform for oncolytic virotherapy. Many clinical VV candidates, such as the double-deleted VV, vvDD, are engineered with deletions that enhance viral tumor selectivity based on cellular proliferation rates. An alternative approach is to exploit the dampened interferon-based innate immune responses of tumor cells by deleting one of the many VV immunomodulatory genes expressed to dismantle the antiviral response. We hypothesized that such a VV mutant would be attenuated in non-tumor cells but retain the ability to effectively propagate in and kill tumor cells, yielding a tumor-selective oncolytic VV with significant anti-tumor potency. In this study, we demonstrated that VVs with a deletion in one of several VV immunomodulatory genes (N1L, K1L, K3L, A46R, or A52R) have similar or improved *in vitro* replication, spread, and cytotoxicity in colon and ovarian cancer cells compared to vvDD. These deletion mutants are tumor selective, and the best performing candidates (ΔK1L, ΔA46R, and ΔA52R VV) are associated with significant improvement in survival, as well as immunomodulation, within the tumor environment. Overall, we show that exploiting the diminished antiviral responses in tumors serves as an effective strategy for generating tumor-selective and potent oncolytic VVs, with important implications in future oncolytic virus (OV) design.

INTRODUCTION

The genetic alterations commonly found in tumors that produce uncontrolled growth and survival can establish a highly favorable environment for viral propagation.[1] This creates engineering opportunities to design tumor-selective oncolytic viruses (OVs) that are effective, targeted anti-cancer agents. When infecting normal cells, viruses express modulatory proteins that facilitate viral replication and evasion of host immune responses.[2–5] However, many tumor cell types already have a disrupted immune response[6] and a higher pool of nucleotides[7] associated with their rapid growth. Thus, the action of many viral virulence factors in the context of malignant cell infection may be redundant. This forms the basis of strategies aimed at enhancing the tumor selectivity of OVs, through the deletion of genes necessary for infection of normal cells but superfluous in the tumor environment.[6,8,9]

Vaccinia virus (VV) has a variety of characteristics that make it an optimal OV platform. These include a large double-stranded DNA genome (200+ genes), which can be easily engineered by standard DNA manipulation techniques,[10] an exclusively cytoplasmic life cycle,[11] broad host tropism,[12] and an extensive history of clinical use demonstrating safety in humans.[13,14] As anti-cancer agents, current oncolytic VV candidates have demonstrated safety and encouraging initial efficacy in clinical trials. For instance, treatment with JX-594, a Wyeth strain VV with deletion of the thymidine kinase (TK) gene and a granulocyte-macrophage colony-stimulating factor insertion, was associated with an overall survival of 14.1 months compared to 6.7 months in patients with advanced hepatocellular carcinoma when given intratumorally at 1×10^9 PFU compared to 1×10^8 PFU, respectively.[15] Double-deleted VV (vvDD), a Western Reserve strain with deletions in TK and vaccinia growth factor (VGF), has shown similarly encouraging results in advanced melanoma. Intratumoral treatment with 3×10^9 PFU, for instance, has been associated with viral replication in both injected and non-injected lesions with sparing of normal tissue.[16] These initial results are encouraging, but improved anti-tumor effect will be necessary to advance the clinical efficacy of VV moving forward. Given the significant attenuation of vvDD and its potential limited effect for instance in slow-growing tumors, we aimed to develop safe and efficacious oncolytic VVs using an alternate strategy to exploit the rapid growth of tumors.

Many OVs advancing through clinical trials, including vvDD and JX-594, have enhanced tumor specificity due to the proliferative nature of malignant cells compared to their normal counterparts. This mechanism of tumor selectivity is achieved through gene deletions that render viruses reliant on the host cell's supply of nucleotides.[8,17] While this strategy is effective for fast-growing tumors with large

Received 9 October 2020; accepted 12 May 2021;
https://doi.org/10.1016/j.omto.2021.05.007.

[4]Present address: Lunenfeld-Tanenbaum Research Institute, Mount Sinai Hospital, Toronto, ON, Canada

Correspondence: Dave Mealiea, Toronto General Hospital Research Institute, University Health Network, 280 Elizabeth Street, Toronto, ON M5G 2C4, Canada.
E-mail: d.mealiea@mail.utoronto.ca

Table 1. Candidate VV immunomodulatory gene roles

VV gene	Role
N1L	Inhibits NF-κB and IRF3 activation via interaction with the IKK (complex) and TBK1[52]
	Inhibits pro-apoptotic proteins (Bad/Bax/Bid) by binding to their BH3 motifs[38]
K1L	Prevents regulatory protein IκBα degradation and subsequent release of NF-κB into the nucleus,[53] blocks early and intermediate viral RNA from triggering PKR-dependent NF-κB activation,[54] and inhibits acetylation of NF-κB subunit RelA[55]
	Binds to ACAP2[56]
	Acts as a host range protein[57]
K3L	Prevents the inhibition of host protein translation by inhibiting PKR activity by preventing autophosphorylation of PKR and phosphorylation by eIF2α[58]
A46R	Inhibits TLR and IL-1 signaling by binding to TIR-domain-containing proteins (i.e., MyD88, TRIF, MAL, TRAM) thereby inhibiting NF-κB, MAPK, and IRF3 activation[20]
A52R	Inhibits TLR and IL-1 signaling by binding to IRAK2 and TRAF6[59]
	Activates p38 MAPK to drive TLR-4 mediated IL-10 expression[21]
	Activates MAPK/AP-1 (c-Jun) pathway[39]

Abbreviations: IRF3, interferon-regulatory factor 3; IKK (complex), IκB kinase (complex); BH3, B cell lymphoma 2 homology 3; PKR, protein kinase R; eIF2α, α subunit of eukaryotic initiation factor 2; IL-1, interleukin-1; TIR, Toll/IL-1 receptor; MyD88, myeloid differentiation factor 88; TRIF, Toll-receptor-associated activator of interferon; MAL, MyD88 adaptor-like protein; TRAM, TRIF-related adaptor molecule; MAPK, mitogen-activated protein kinase; IRAK2, IL-1-receptor-associated kinase 2; TRAF6, tumor-necrosis-factor-receptor-associated-factor 6; AP-1, activator protein 1.

nucleotide pools, it is not optimal for slow-growing malignancies and fails to capitalize on the dysfunctional antiviral response that characterizes many tumor cells.[6]

VV expresses several immunomodulatory genes to evade the host immune response,[5,18] and single or multiple gene deletions may attenuate its ability to replicate in non-tumor cells without affecting its virulence in transformed cells. Using the Western Reserve VV strain, which has enhanced tumor specificity and anti-tumor potency at baseline,[19] we generated a panel of oncolytic VVs with gene deletions related to the inhibition of host cell interferon (IFN) induction and signaling pathways. These included N1L, K1L, K3L, A46R, and A52R. Previous studies have suggested that single gene deletions of A46R, A52R, N1L, and K1L lead to reduced virulence in BALB/c mice compared to the parent VV backbone.[20–25] When K3L was deleted, viral replication was maintained in HeLa cells, but not BHK cells.[26] As such, we postulated that a single gene deletion of N1L, K1L, K3L, A46R, or A52R from Western Reserve VV would generate a tumor-selective oncolytic virus with improved tumor-potency compared to vvDD.

RESULTS

Creation of candidate VV deletion mutants

In order to determine whether VVs with a dampened ability to block type I IFN responses would exhibit tumor-specific replication and potent oncolytic activity, we generated a panel of Western Reserve VVs with a deletion in one of several VV immunomodulatory genes. These included N1L, K1L, K3L, A46R, or A52R. Gene candidates were rationally selected based on their role in inhibiting major steps in IFN induction and signaling pathways (Table 1). Homologous recombination was facilitated by flanking an expression cassette with DNA sequences associated with each gene of interest. Primers (Table 2) were designed based on gene sequences described in GenBank accession number AY243312. The resultant candidate VV deletion mutants have each immunomodulatory gene interrupted by an expression cassette containing the R2R segment and a xanthine-guanine phosphoribosyltransferase (xgprt) gene (Figure 1). Viruses were confirmed by red fluorescent protein (RFP) expression and PCR (data not shown).

Candidate VV deletion mutants exhibit cytotoxicity, replication, and spread similar to or better than vvDD in monolayers of colon and ovarian cancer cell lines

The *in vitro* oncolytic potential of our candidate VV deletion mutants was compared to vvDD[16,27] in terms of tumor cell cytotoxicity, viral replication, and viral spread in MC38, DLD-1, and A2780 cancer cell lines. Cytotoxicity was measured using the 3-(4,5-dimethyl-2-yl)-5-(3-carboxymethoxyphenyl)-2-(4-sulfophenyl)-2H-tetrazolium (MTS) assay in monolayer cultures infected at an MOI of 1. The cytotoxicity of each of our candidate VV deletion mutants was either equal to or higher that of vvDD in the colon cancer cell lines MC38 and DLD-1 (Figure 2). The difference in cytotoxicity of all candidate VVs compared to vvDD was most dramatic in MC38 cells, where cell viability of samples infected with candidate VVs was reduced to approximately half that of vvDD-treated cells at 72 hpi ($p < 0.05$; Figure 2A). Ovarian cancer A2780 cells were the most susceptible to all VVs, where the relative survival was less than 50% by 48 h in all treatment groups (Figure 2C). Among all candidate VV deletion mutants, the ΔA46R VV was the most cytotoxic with a mean cell viability of 40.1% ± 0.3%, 40.3% ± 2.0%, and 4.8% ± 1.1% at 72 h in MC38, DLD-1, and A2780 cells, respectively. While some of the difference in cytotoxicity may be explained by the presence of TK and VGF genes, the fact that there was significant variation in replication and spread between candidate VVs (Figures 2G–2I and 3A and 3B) as described below, and that the most cytotoxic candidates did not display the highest replication levels, suggests other mechanisms were likely at play as well.

Table 2. Primers for producing inserts for the shuttle plasmid

Gene		Left flanking insert	Right flanking insert
N1L	Fwd	5′-gatccaattg cctaactctt tcgaatactt-3′	5′-gatcgcgcgcgtacatacatcgccgtcatc-3′
	Rev	5′-gatcgctagc ggaagagtca ttcaccatac-3′	5′-gatccagctgttatggaggatatgtgaacgc-3′
K1L	Fwd	5′-gatccaattgtgacgtacatgagtctgagt-3′	5′-gatcgcgcgctttgcatgttaccactatca-3′
	Rev	5′-gatcgctagccgtggatatgatgattctct-3′	5′-gatccagctgcagacatggatctgtcacga-3′
K3L	Fwd	5′-gatccaattgtaccggatctacgttctact-3′	5′-gatcgcgcgcataatccttctcgtatac-3′
	Rev	5′-gatcgctagcggatatatagatgtcaatta-3′	5′-gatccagctgtgctgatcctcccattccgt-3′
A46R	Fwd	5′-gatccaattgcacgataatatcagaggagt-3′	5′-gatcgcgcgctgacttacttgtataataag-3′
	Rev	5′-gatcgctagccttcattacgtatgactaat-3′	5′-gatccagctgcagaacatgtagacgaatca-3′
A52R	Fwd	5′-gatccaattgcgggagacgaggatatagct-3′	5′-gatccccgggacgcgtgacaatgatgcggaagaaca-3′
	Rev	5′-gatccccgggaggcctatagacctctgtacataaaa-3′	5′-gatcgacttgagcgtcatctggtagatagaccatcg-3′

Abbreviations: Fwd, forward; Rev, reverse.

The replication and spread of the VVs in all cancer cell lines were assessed by infecting cancer cells at a low MOI of 0.1. The replication of vvDD and VV deletion mutants in all cell lines resulted in a 2–3 log-fold increase in total virus by 72 hpi (Figures 2D–2I). In general, all candidate VV deletion mutants exhibited similar or better viral replication compared to vvDD in MC38, DLD-1, and A2780 cells at peak viral titers, with the exception of ΔA46R VV (Figures 2D–2I). However, the replication efficiency of all VVs in A2780 cells was generally higher compared to the colon carcinoma cells (Figure 2G–2I). Among them, the ΔK1L VV demonstrated the most efficient replication ability across all cell lines, with the average fold change in replication being 2.8, 13.9, and 2.3 times higher than the average fold change of vvDD in MC38, DLD-1, and A2780 cells, respectively (Figures 2G–2I, $p < 0.05$).

The spread of all candidate VVs was similar or better than vvDD in all cell lines tested, as confirmed by both visual assessment and quantitative analysis (Figure 3). Visual assessment confirmed superior viral spread for ΔK1L VV, ΔN1L VV, and ΔA52R VV in all cell lines. The best performer, ΔA52R VV, demonstrated consistently significant superior viral spread in all cell lines, infecting 55.6% ± 6.1%, 39.7% ± 8.5%, and 65.5% ± 4.1% of monolayers of MC38, DLD-1, and A2780 cells, respectively (Figure 3). As such, mean ΔA52R VV spread was 11.8%–33.7% better relative to vvDD at peak time points in all tested cell lines (Figure 3, $p < 0.05$).

Candidate VVs exhibit equal or better viral spread and cytotoxicity in tumor spheroids compared to vvDD

We used MC38 and DLD-1 tumor spheroids to mimic the 3D structure and microenvironment of a tumor mass and allow for more relevant *in vitro* investigation[28] (Figure 4). At 72 hpi, the majority of infection was concentrated at the spheroid periphery. In comparing vvDD to candidate viruses, only minimal amounts of RFP expression associated with vvDD infection could be seen in MC38 spheroids at 72 hpi. In contrast, the ΔN1L, ΔK1L, ΔA46R, and ΔA52R VVs infected most of the rim and exhibited some penetration into the MC38 spheroids. The DLD-1 spheroids were more resistant to infection by VVs, resulting in small, dispersed foci of RFP by 72 hpi. However, ΔA52R VV was able to infect a larger portion of the DLD-1 spheroids. Out of all viruses tested, ΔA52R VV demonstrated the most substantial spread in both MC38 and DLD-1 spheroids (Figure 4A). Moreover, virus-induced cytotoxicity of all VVs resulted in $\leq$3.3% and $\leq$1.3% surviving fraction in MC38 and DLD-1 spheroids, respectively, at 96 hpi as measured by a clonogenic assay (Figures 4B and 4C).

At therapeutic doses, candidate VV's have preserved tumor specificity and significant survival benefit

The 3 best-performing candidate VVs *in vitro* were chosen for subsequent *in vivo* investigation against vvDD. These were ΔK1L VV, ΔA46R VV, and ΔA52R VV.

Maximum tolerable doses (MTDs) were determined by injecting increasing doses of VV intraperitoneally (i.p.) into non-tumor-bearing mice. The highest dose at which mice survived for 4 weeks or more was deemed the maximum tolerable dose and used for subsequent tumor survival studies (data not shown). For immunocompetent C57BL/6 mice, the i.p. MTD for the ΔK1L VV was 5×10^7 PFU, while the MTD of ΔA46R VV and ΔA52R VV was 1×10^7 PFU. The i.p. MTD of all candidate VVs in nude mice was 10^6 PFU. In contrast, the established i.p. dose of vvDD is 10^9 PFU, where only transient weight loss after injection is observed.[8,29]

The anti-tumor efficacy and tumor-selectivity of i.p.-delivered candidate VVs and vvDD were compared in tumor-bearing models of PC. Specifically, a syngeneic model of C57BL/6 mice bearing i.p. MC38 tumors and xenograft models in nude (NU/NU) mice bearing i.p. A2780 or DLD-1 tumors were used. Mice were injected i.p. with tumor cells and treated with i.p. VV 12 days later at indicated doses.

Using the MTD for each virus to evaluate clinically relevant anti-tumor efficacy, candidate VV deletion mutants improved survival similar to or better than vvDD with respect to mock-treated controls. In the MC38 tumor-bearing C57BL/6 syngeneic model (Figure 5A),

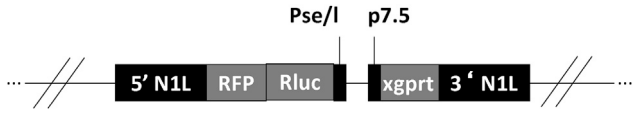

Figure 1. Sample linear diagram of candidate VV DNA insert

Upstream and downstream DNA segments of the deleted gene (N1L in the example) flank the (1) R2R segment consisting of RFP conjoined to Renilla luciferase by a foot-and-mouth-disease virus 2A motif (Rluc) under the synthetic early/late promoter Pse/I and (2) xanthine-guanine phosphoribosyltransferase (xgprt) gene under regulation of the p7.5 promoter. The ΔN1L VV is illustrated above but all other candidate VVs (ΔK1L, ΔK3L, ΔA46R, and ΔA52R) contain the same constructs flanked by the corresponding gene segments.

vvDD- and ΔA46R-treated mice showed a trend toward improved survival over mock-treated mice. On the other hand, a significant improvement in median survival time compared to mock-treated mice was observed in ΔK1L-treated mice (35 days v.s. 28.5 days, $p = 0.0058$), not observed in vvDD, and ΔA52R VV-associated median survival was also longer than vvDD or mock treatment (32.5 days).

There was a trend toward improved survival over vvDD in xenograft models of PC using DLD-1 tumor-bearing mice (Figure 5B), with long-term survival at 160 dpi observed in 12.5%, 25%, and 37.5% of vvDD-, ΔA46R VV-, and ΔA52R VV-treated mice, respectively. Finally, in A2780 tumor-bearing mice (Figure 5C), ΔK1L VV treatment, unlike vvDD or the other candidate VVs, significantly improved median survival time compared to mock-treated mice (53.5 days versus 40 days, $p = 0.0021$). A 12.5% long-term survival rate was associated with vvDD, ΔK1L, and ΔA52R treatment.

VV replication preferentially targeted the tumor and the ovaries in all cancer mouse models tested (Figure 6). In C57BL/6 mice bearing MC38 tumors (Figure 6A), 2–4 log-fold less candidate VV deletion mutant titer was detected in the tumor compared to vvDD. With the exception of the ovaries, all viruses displayed several log-fold titer reductions in other non-tumor tissues compared to tumor. Most impressively, ΔA52R VV was undetectable in the bowel, spleen, liver, heart, and brain. In DLD-1 and A2780 tumor-bearing NU/NU mice (Figures 6B and 6C), the tumor viral load of candidate VVs compared to vvDD was more similar, ranging within approximately 1 log of each other. In general, the concentration of infectious particles of all candidate VV deletion mutants and vvDD was lower in non-tumor tissues, except the ovary, compared to tumor.

Candidate VVs and vvDD treatment are associated with increased immune infiltration into tumors

A portion of the tumors harvested from the MC38 and DLD-1 tumor mouse models were used for immunohistochemistry and stained for B220 (B cells), CD3 (T cells), F4/80 (macrophages), and Ly6G (neutrophils/PMN-MDSC's; Figure 7). There were no significant differences in B220 staining between all treatment groups for both tumor models (Figure 7A) whereas all candidate VVs were associated with increased T cell infiltration into MC38 tumors (ΔK1L VV, 7.18% ± 0.78%; ΔA46R VV, 6.79% ± 0.81%; ΔA52R VV, 9.96% ± 0.30%) compared to mock-treatment (0.15% ± 0.06%), but not vvDD (3.56% ± 0.89%; Figure 7B). Moreover, the percent F4/80 staining in MC38 tumors treated with ΔA52R VV was at least 3 times higher than both mock- and vvDD-treated tumors. Similarly, ΔA52R VV treatment in DLD-1 tumors was associated with an increased mean percent of F4/80 staining compared to mock treatment (Figures 7C and 7E). In contrast, no increase in neutrophil/MDSC infiltration was seen with any of the viruses compared to mock (Figure 7D); however, there was a significant decrease seen in ΔK1L VV compared to vvDD.

DISCUSSION

Genetic alterations in tumor cells can disrupt host antiviral pathways and render immunomodulatory viral genes redundant for successful viral infection and propagation. Mutations affecting IFN responses are common in tumors, with an estimated 65%–70% of cancer cell lines harboring defective IFN responses.[6] Other groups have designed OVs to exploit this phenomenon. For example, Kirn et al.[30] investigated a VV with a deletion in its IFN-β antagonist, B18R, as a potential oncolytic VV. Here, we describe a panel of Western Reserve VVs with a gene deletion in a VV antagonist of TLRs (A46R, A52R), nuclear factor-κB (NF-κB; N1L, K1L), or PKR (K3L; Table 1). To assess the potential of these VVs as oncolytic agents, we compared the candidate VVs to a clinical candidate oncolytic VV, vvDD.[16,27] We hypothesized that our panel of VVs with single VV immunomodulatory gene deletions would have improved potency against colon and ovarian cancer while retaining equal or better attenuation in normal tissue compared to vvDD.

Overall, the candidate VVs performed equally or better than vvDD in our *in vitro* assessments in terms of cytotoxicity, replication, and spread in the colon cancer cell lines MC38 and DLD1, and the ovarian cancer cell line A2780. These cell lines have been found to be moderately to poorly responsive to IFN.[30–35] Interestingly, the ΔK1L, ΔA46R, and ΔA52R VV consistently demonstrated superior viral replication, tumor cytotoxicity, and viral spread. This suggests that the redundancy of the deleted IFN-related genes in cancer cells may indeed support VV propagation and cell-killing *in vitro*, although further investigation, for instance comparing IFN-deficient and IFN-intact tumor cell lines, is needed. The deletions in vvDD (TK and VGF) render the virus reliant on the cell-intrinsic pool of nucleotides[8] while the candidate VVs still express TK and VGF. This may be problematic for vvDD spread within the tumor environment, reflected here in tumor spheroids, where, for example, the nutrient gradient renders tumor cells near the center of the spheroid quiescent.[33] However, vvDD can better defend itself against host cell antiviral mechanisms as it still expresses the full armamentarium of VV immunomodulatory genes.

The improved performance of candidate VV's over vvDD *in vitro* may speak to both the presence of TK and VGF genes and the comparative degree of reduced fitness that results from immunomodulatory gene deletion as opposed to TK and VGF deletions. Given that

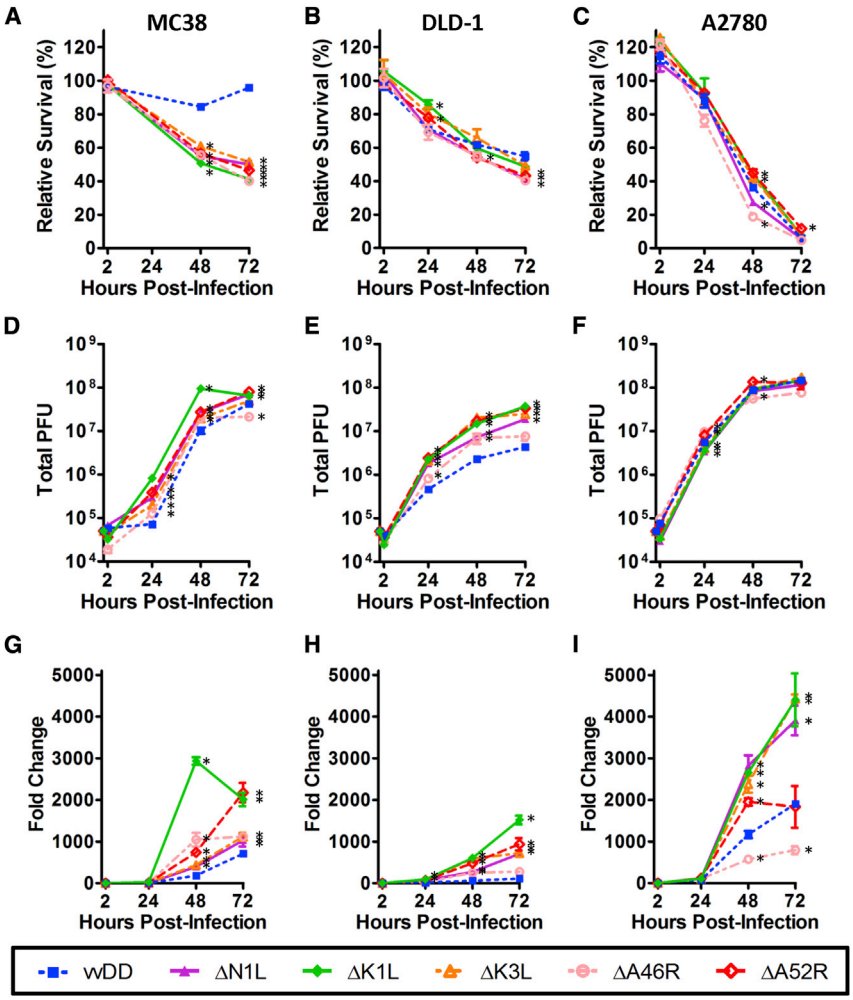

Figure 2. VV replication and cytotoxicity in tumor cell lines

(A–C) Monolayers of tumor cell lines were mock-infected or infected with either vvDD or one of the candidate deletion mutants at an MOI of 1 (n = 3). Cell viability is presented as absorbance relative to mock as measured by an MTS assay. (D–I) Monolayers of tumor cell lines were mock-infected or infected with either vvDD or a candidate VV deletion mutant at an MOI of 0.1 (n = 3). Data represent (D–F) viral load and (G–I) fold change relative to baseline PFU at 2 hpi. Values are means of triplicates ± SEM corresponding to a representative experiment out of three independent experiments. *p < 0.05 compared to vvDD.

we demonstrated variability in the *in vitro* activity of each candidate VV, this would support a role for the redundancy of VV IFN genes in these tumor cell lines above and beyond only the presence of TK and VGF. However, further investigation into the complex interactions between VV and host cells is necessary to more fully explain the observed phenomena.

The ΔA46R VV demonstrated superior *in vitro* tumor cytotoxicity as measured by the MTS assay. The product of the A46R gene, A46, inhibits TLR signaling through Toll/interleukin 1 receptor (TIR) domain-containing proteins, ultimately decreasing NF-κB, IFN regulatory factor 3 (IRF3), and mitogen-activated protein kinase (MAPK) activation.[20] Among the protein targets of A46, TIR-domain-containing adaptor-inducing IFN-β (TRIF) can induce apoptosis through a protein motif that can also activate NF-κB.[34] Thus, we hypothesize that the deletion of A46R enables TRIF-induced apoptosis in response to the VV infection leading to the higher cell death compared to other candidate VVs and vvDD. While a deeper investigation of the molecular mechanisms at play here was outside the scope of this study, further evaluation of specific VV deletion mutants is planned to confirm the degree to which changes in components of the IFN pathway such as TRIF and types of tumor cell death are involved.

The ΔK1L VV consistently replicated to the highest titer within 72 h following *in vitro* infections. While constitutive expression of NF-κB is characteristic of many tumor types, including the cell lines used in this study,[35–40] other common perturbations in malignant cells such as Ras/MEK activation nonetheless suppress downstream expression of various IFN response genes.[32] Based on the above findings for our ΔK1L VV, one explanation is that this gene is the most redundant in the face of this repression of IFN response in the tumor lines evaluated.

Among the two genes with direct effects on NF-κB, N1L also has anti-apoptotic properties,[38] which may be important for prolonging host cell survival to allow more VV replication. Thus, we hypothesize that the K1L was the most redundant VV gene among our candidate genes for enhancing VV replication in monolayer cultures of tumor cells, leading to the superior viral replication seen compared to candidate VVs and vvDD.

Lastly, the ΔA52R VV demonstrated the best *in vitro* spread for all cell lines in both monolayer and spheroid culture. In addition to inhibiting TLR signaling, the expression of A52R leads to c-Jun N-terminal kinase (JNK)[21] and AP-1 activation.[39] During VV infection, JNK activation is important for cytoskeleton reorganization. In JNK1/2 knockout cells, early cell contractibility in response to Western Reserve (WR) VV infection is abrogated and plaque size, trafficking of early virions to the cell periphery, and the number of extracellular enveloped virions released are increased.[40] Thus, the reduced JNK activation during ΔA52R VV infection may lead to increased extracellular enveloped virus (EEV) release, thereby increasing VV spread. Pereira et al.[40] hypothesized that WR VV induces cytoskeleton rearrangements in order to congregate immature virions and

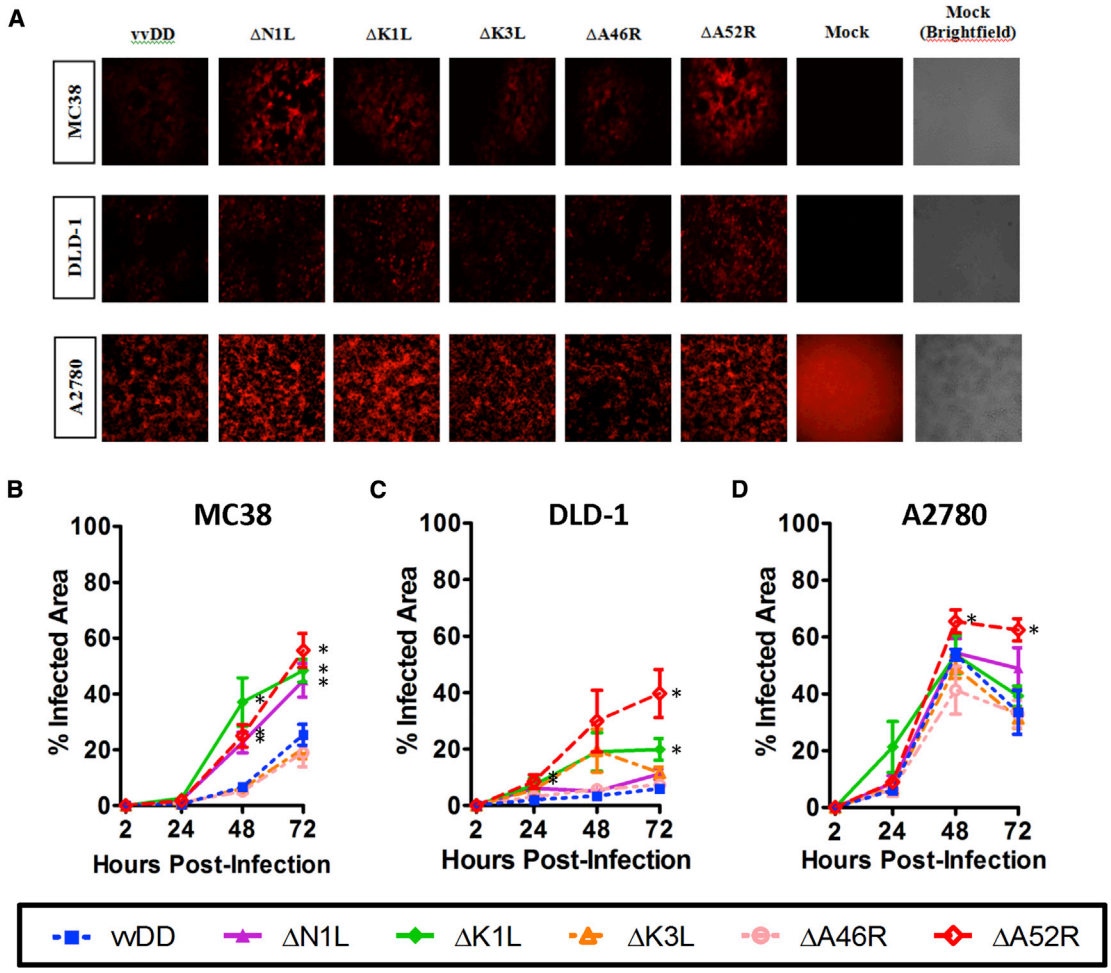

Figure 3. VV spread in monolayer tumor cell lines

Tumor cell lines were mock-infected or infected with either vvDD or a candidate VV deletion mutant at an MOI of 0.1 and evaluated for viral spread based on RFP marker expression. (A) Representative bright-field and fluorescent images (Cy3) at 10× magnification at peak fluorescence at 72 hpi (MC38, DLD-1) or 48 hpi (A2780; n = 3). (B–D) Quantification of percent infected area (n = 3). Data are a combination of two independent experiments, each with three replicates, and values are mean ± SEM. *p < 0.05 compared to vvDD.

reduce immune detection by the host, thereby increasing VV replication and spread. Perhaps this mechanism is redundant in our tumor cell lines and the possible increase in EEV release in the absence of A52R provided more benefit.

We subsequently investigated our top performing candidate VVs (ΔK1L, ΔA46R, and ΔA52R VVs) from our *in vitro* studies in mouse models of peritoneal carcinomatosis. At doses that would likely be used in the clinical setting, the tumor selectivity of our candidate VVs was similar to vvDD. In agreement with literature,[8,29,41] the viral replication of vvDD localized to the tumors and ovaries. Likewise, the candidate VVs showed a similar biodistribution in all mouse models. Both engineered and intrinsic properties of VV would have contributed to the biodistribution of candidate VV and vvDD replication. The deletions in candidate VVs dampen their ability to inhibit host innate antiviral mechanisms, allowing normal tissues to more effectively defend against successful candidate VV propagation compared to tumor cells, which often have defective antiviral responses. Intrinsically, VVs are large viruses; hence, the virions may accumulate in tissues with leaky vasculature that allow VV to exit the bloodstream, such as tumors.[42] Though the viral load in the ovaries for all VVs was high, this may be a mouse-specific phenomenon as vvDD was undetectable in non-human primate ovaries 6 days following intravenous (i.v.) treatment.[43] Further, the amount of replicating WR VV found in the ovaries of rhesus macaques (3,646 PFU/mg) was comparably lower than the viral load of candidate VVs in our mouse ovaries.[43] A possible explanation is that the estrous cycle in mice, involving periods of increased cell proliferation and angiogenesis in mouse ovaries,[44] contributed to the high VV load in our models.

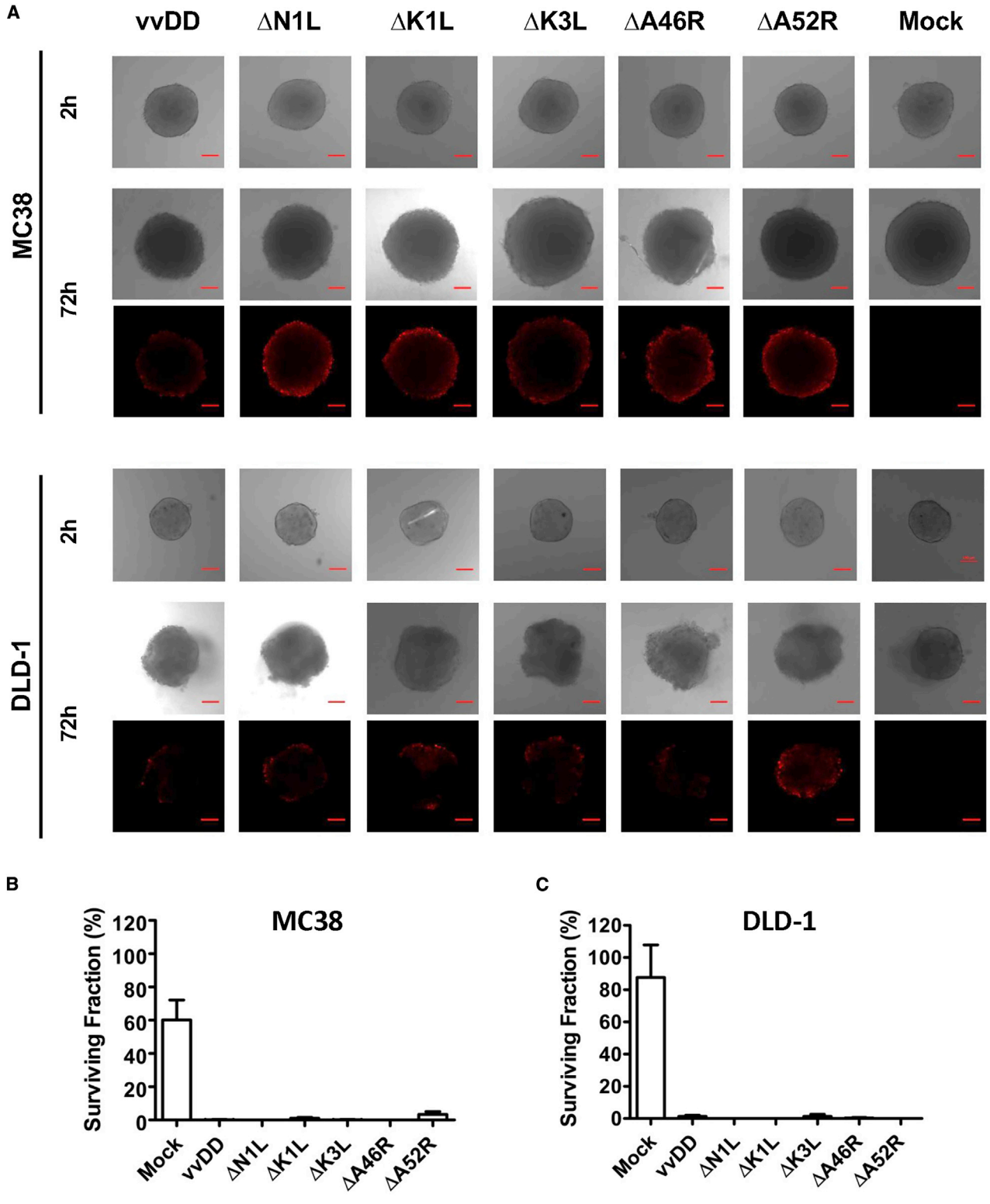

(legend on next page)

Treatment with the candidate VVs demonstrated a survival benefit in both immunocompetent and immunocompromised tumor-bearing mouse models at dosages chosen through MTD determination. The maximum doses at which non-tumor-bearing mice survived 4 weeks following infection were deemed treatment doses for survival studies (data not shown). Compared to the established vvDD dose of 10^9 PFU, candidate VV treatment doses were 20–100 times lower in C57BL/6 mice (ΔK1L VV, 5×10^7 PFU; ΔA46R and ΔA52R VV, 1×10^7 PFU) and 1,000 times lower in NU/NU mice (1×10^6 PFU). Lower MTDs of the candidate VVs were expected. Unlike vvDD, the deletions in the VV immunomodulatory genes render our candidate VVs unable to inhibit the antiviral signaling cascade leading to pro-inflammatory cytokine and IFN activation. Possibly, a cytokine storm in response to the candidate VV infection resulted in a heightened immune response that contributed more to the tissue damage and subsequent deaths than the VV infection alone. Further studies measuring cytokine and IFN induction following candidate VV treatment will be necessary to confirm this speculation. Nonetheless, given our biodistribution and anti-tumor data for candidate VVs, the reduced dosing compared to vvDD appears to be both safe and effective at this initial stage of evaluation.

In our MC38-bearing immunocompetent model, only the ΔK1L VV treatment was associated with a statistically significant improvement in median survival compared to mock ($p = 0.0058$). Moreover, the viral load in tumors was the lowest among mice in the ΔK1L-treated group by 6 days post-treatment. It is well-established that OVs have multiple mechanisms of action against cancer including direct oncolysis, disruption of vasculature, and induction of anti-cancer immunity.[45] Immunohistochemistry results show that ΔK1L VV treatment increased T cell infiltration compared to mock-treatment even though neutrophil and MDSC infiltration was decreased compared to vvDD treatment in this model. This is similar to the intradermal ΔK1L VV infection model by Cruz et al.[25] wherein innate immune cell infiltrate decreased but VV-specific $CD8^+$ T cell infiltration and activation were elevated compared to wild-type WR VV. Thus i.p. ΔK1L-VV treatment in our immunocompetent mice may have also resulted in improved tumor-specific adaptive T cell response, which contributed, in conjunction with direct viral lysis, to the improved anti-tumor efficacy.

Similar to findings associated with the NYVAC VV strain,[46,47] our ΔA46R and ΔA52R WR VV treatments also increased T cell infiltration into tumors. However, these vectors offered no statistically significant improvement in the median tumor survival compared to mock- and vvDD-treated groups. Perhaps the initial higher replication efficiency of ΔK1L VV demonstrated in the *in vitro* assays was translated to this mouse model and triggered a more robust anti-cancer immune response with more T cell activation compared to ΔA46R VV, ΔA52R VV, and vvDD. A more in-depth investigation of the immune response will be necessary to uncover the mechanism of anti-tumor efficacy of the candidate VVs in an immunocompetent model.

Candidate VVs also improved the survival of nude mice implanted with human ovarian or colon cancer xenografts. In DLD-1 tumor-bearing mice, the ΔA52R VV treatment was associated with complete response and long-term survival in the highest proportion of mice (37.5%), followed by ΔA46R VV (25%) and vvDD (12.5%). There were no differences in immune infiltrates between VVs in DLD-1 tumor-bearing mice except for an increase in $F480^+$ cells in ΔA52R VV-treated tumors compared to the mock treatment. In A2780 tumor-bearing mice, ΔK1L VV improved mean survival, but both ΔK1L and ΔA52R VV treatment conferred complete responses and long-term survival (12.5%). In both models, immunocompromised nude mice were used to allow for human tumor development. Hence, the major contributors of tumor efficacy were potentially direct viral oncolysis, vasculature disruption, and the innate immune response. As in the immunocompetent model, the factors that influenced candidate VV efficacy could also apply to the efficacy observed in the nude mouse models. The superior ΔA52R VV spread, demonstrated in monolayer and spheroid culture, may have played a major role in its therapeutic efficacy in the immunocompromised models, especially in the DLD-1 tumor-bearing mice as DLD-1 is relatively resistant to VV infection and spread.[29] The redundancy of a particular VV gene deletion in promoting successful VV propagation is important for anti-tumor efficacy in these models. In addition, the induction of innate immunity by candidate VV or vvDD infection, though dysregulated in tumor cells,[6] may have also contributed to anti-tumor efficacy. Other groups have investigated innate immune induction from candidate VV gene-deleted vectors and vvDD in different models.[25,46–51] Further work will be necessary to elucidate the innate immune response and cytokine induction in our tumor-bearing nude mouse models and correlate them to the anti-tumor efficacy presented in this study. Finally, in the DLD-1 model, all viruses, including vvDD, demonstrated an early non-significant increased death rate over control treatment. While this may have been due to the increased pro-inflammatory cytokine response discussed above in the candidate VVs, given that this was also present in vvDD suggests otherwise. Certainly, all VV groups in this model also displayed a trend toward improved survival over mock-treated mice, consistent with MC38 and A2780 models.

In summary, we have generated a panel of novel VVs with deletions in VV immunomodulatory genes (N1L, K1L, K3L, A46R, and A52R) and investigated the potential of these vectors as anti-tumor agents compared to vvDD. The candidate VVs demonstrated equal or

Figure 4. VV spread and cytotoxicity in multicellular tumor spheroids

MC38 and DLD-1 tumor spheroids mock infected or infected with either vvDD or a candidate VV deletion mutant at an MOI of 2 (n = 5). (A) Representative bright-field and confocal fluorescent images (Cy3) at 150 μm depth. Scale bar, 100 μm; 10× magnification (n = 4). Clonogenic assay of (B) MC38 and (C) DLD-1 tumor spheroids at 96 dpi. Surviving fraction is the number of colonies (>50) after 10 days of incubation relative to the number originally seeded. Values are means of triplicates ± SEM corresponding to a representative experiment out of 2 independent experiments.

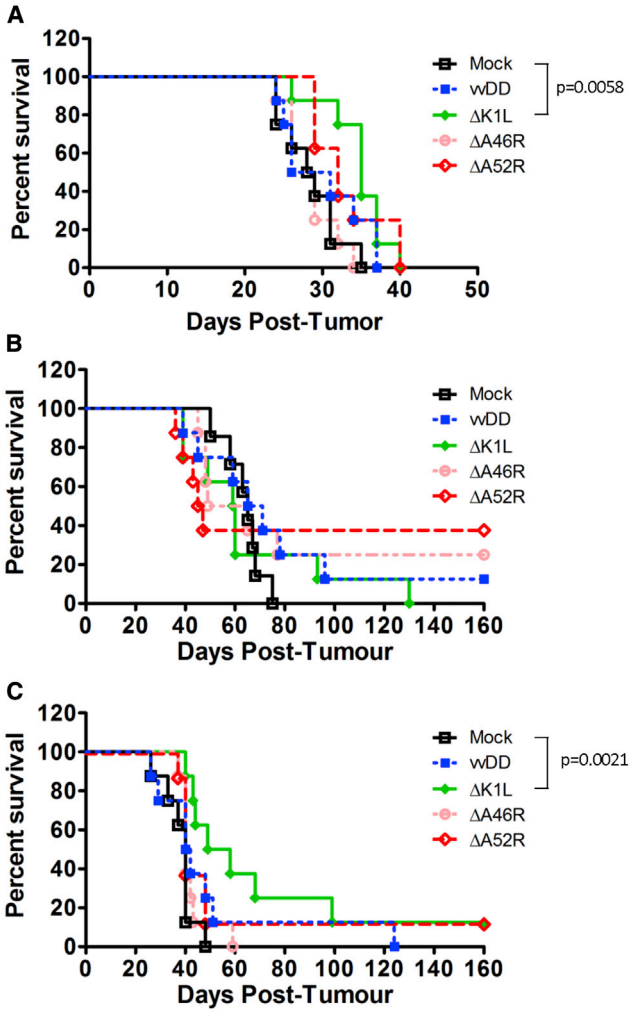

Figure 5. VV tumor efficacy

Mice were injected i.p. with tumor cells and then treated with HBSS alone, vvDD, or a candidate VV deletion mutant (n = 8) 12 days later and followed for survival. Kaplan-Meier curves of (A) MC38-bearing C57BL/6 mice (dose: vvDD = 1×10^9 PFU, ΔK1L = 5×10^7 PFU, ΔA46R = 1×10^7 PFU, or ΔA52R = 1×10^7 PFU), (B) DLD-1-bearing NU/NU mice (dose: vvDD = 1×10^9 PFU, candidate VV deletion mutant = 1×10^6 PFU for all viruses), or (C) A2780 tumor-bearing NU/NU mice (dose: vvDD = 1×10^9 PFU, candidate VV deletion mutant = 1×10^6 PFU). Statistical significance was calculated by log-rank test.

improved *in vitro* viral replication, spread, and tumor cell cytotoxicity in both monolayers and spheroid cultures of colon and ovarian cancer cells. Moreover, superior candidate VVs from the *in vitro* assays (ΔK1L VV, ΔA46R VV, and ΔA52R VV) demonstrated a significant anti-tumor effect, comparable tumor selectivity, and a trend toward improved survival compared to vvDD when using a clinically relevant dosing approach. Thus, we have demonstrated that exploiting the dampened IFN response in tumors is a viable mechanism of tumor selectivity for generating potential OVs. It would be interesting to investigate the interactions between the candidate VVs, tumor, and

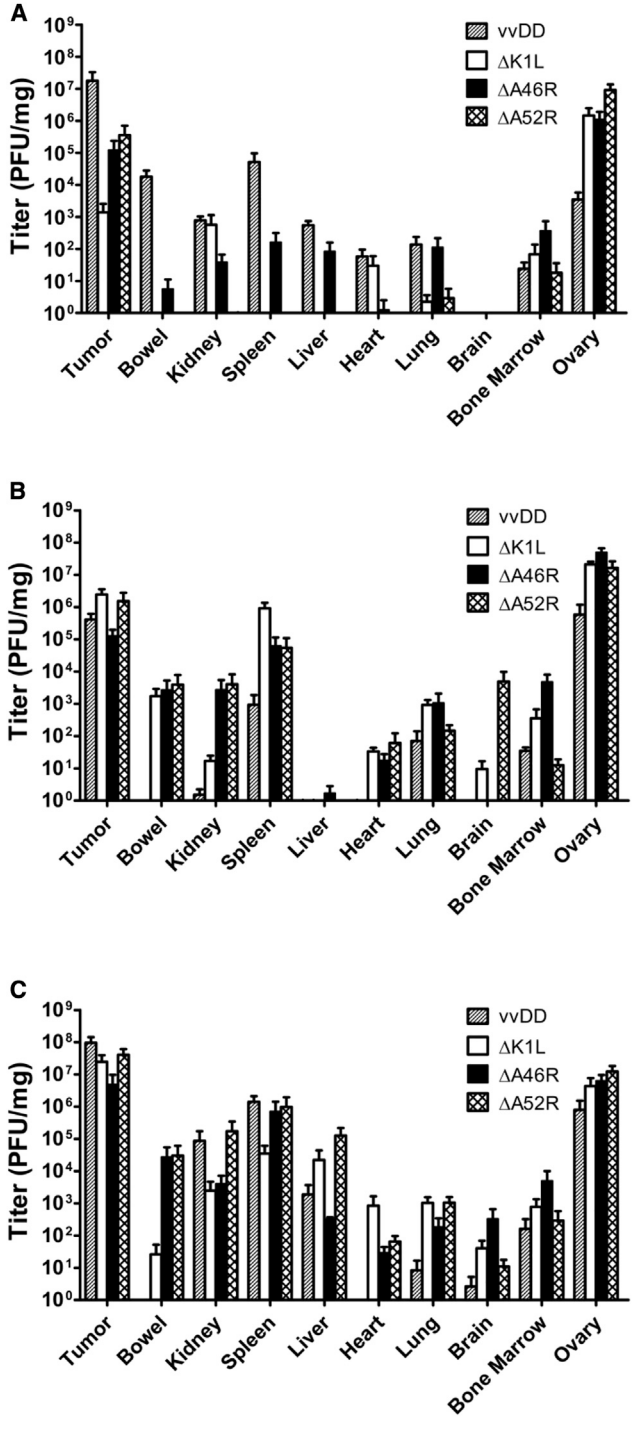

Figure 6. VV tumor selectivity of viral replication

Mice were injected i.p. with tumor cells and then treated with HBSS alone, vvDD, or a candidate VV deletion mutant 12 days later. Tumor and non-tumor tissues were harvested 6 days post-infection (n = 3) and viral load was quantified by plaque assay. (A) MC38-bearing C57BL/6 mice (dose: vvDD = 1×10^9 PFU, ΔK1L = 5×10^7 PFU, ΔA46R = 1×10^7 PFU, or ΔA52R = 1×10^7 PFU), (B) DLD-1-bearing NU/NU mice (dose: all VVs = 5×10^6 PFU), and (C) A2780 tumor-bearing NU/NU mice (all VVs = 5×10^6 PFU). Values are means of triplicates ± SEM.

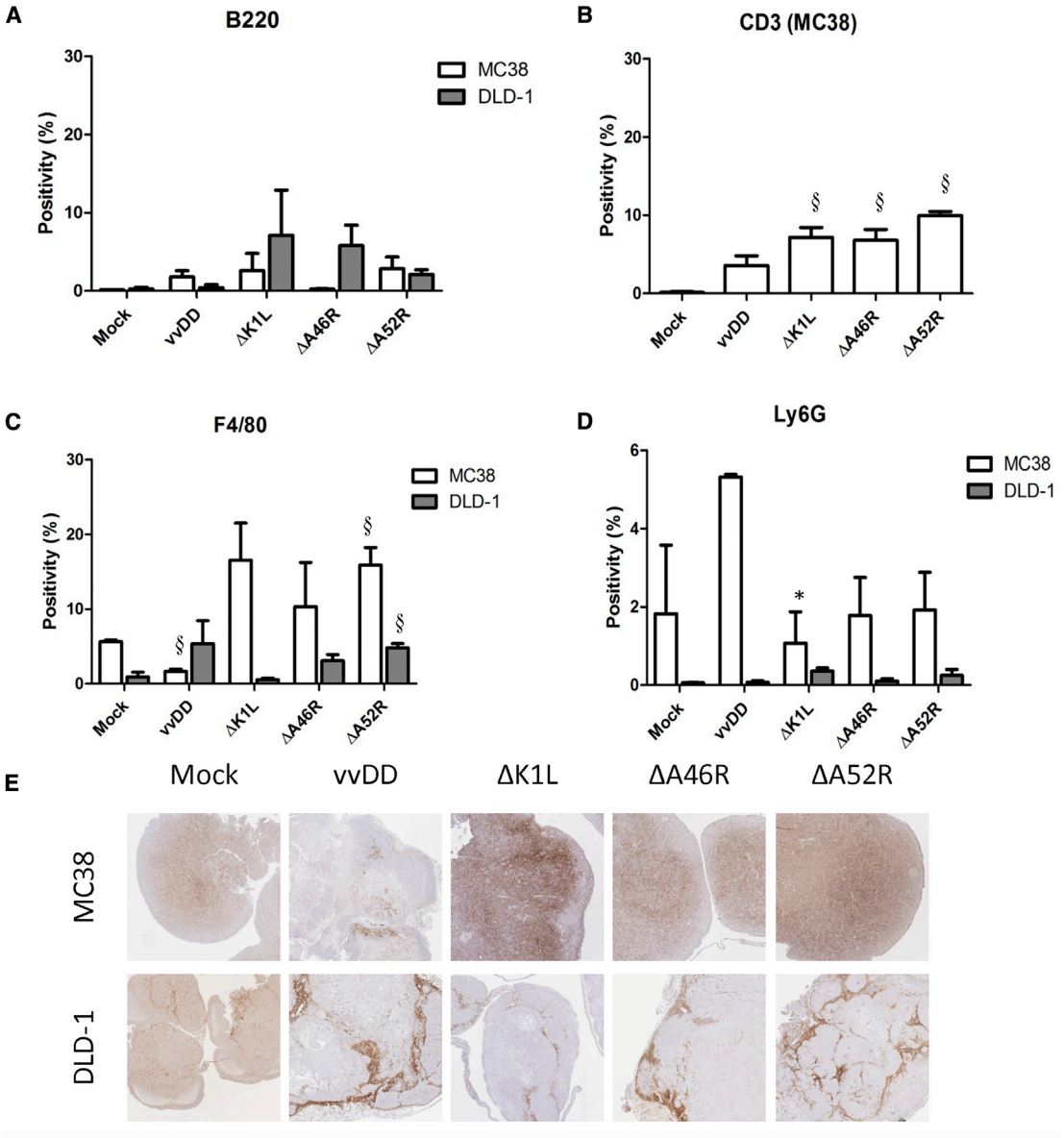

Figure 7. Immune infiltrate of VV-treated tumors

C57BL/6 (n = 3) and NU/NU (n = 3) mice were injected i.p. with MC38 or DLD1 tumor cells, respectively, and treated i.p. with HBSS, vvDD, or candidate VVs 12 days later as follows: MC38-bearing C57BL/6 mice (vvDD = 1×10^9 PFU, ΔK1L = 5×10^7 PFU, ΔA46R = 1×10^7 PFU, or ΔA52R = 1×10^7 PFU), and DLD-1-bearing NU/NU mice (all VVs: 5×10^6 PFU). Mice were sacrificed 6 days post-treatment and 2–3 tumors per mouse were harvested and fixed in formalin for analysis by immunohistochemistry. Quantification of immunohistochemistry staining for (A) B220, (B) CD3 (MC38-bearing C57BL/6 model only), (C) F4/80, and (D) Ly6G. Data depict percent of positively stained pixels relative to total number of pixels per tumor. (E) Representative images of tumors stained for F4/80. Values are means of triplicates ± SEM, §$p < 0.05$ compared to mock-treated (HBSS); *$p < 0.05$ compared to vvDD-treated.

the immune system that lead to improved therapeutic efficacy. A better understanding of the mechanisms would inform possible combination treatments to further improve survival. Additionally, our findings support further investigation of anti-tumor potency of the candidate VVs in other common malignancies. Overall, the immunomodulatory gene deleted VVs described herein are promising OVs for development as clinical cancer therapies.

MATERIALS AND METHODS

Cell lines

Human colorectal adenocarcinoma cell line DLD-1, human ovarian cancer cell line A2780, and normal monkey kidney fibroblast cell line CV-1 were obtained from the American Type Culture Collection (ATCC; Manassas, VA, USA). MC38 murine colorectal adenocarcinoma cell line and C57BL/6 murine sarcoma cell line 24JK were

obtained from the National Institutes of Health (NIH; Bethesda, MD, USA). Cells were cultured at 37°C and 5% CO_2 in media supplemented with 10% fetal bovine serum (FBS; PAA Laboratories, Etobicoke, ON, Canada) and 1% penicillin-streptomycin (Invitrogen, GIBCO, Grand Island, NY, USA). All cell lines were maintained in Dulbecco's modified Eagle's medium (DMEM; Sigma-Aldrich, St. Louis, MO, USA) with the exception of A2780 cells, which were maintained in Roswell Park Memorial Institute medium (RPMI 1640; in-house Toronto Medical Discovery Tower media, University Health Network, Toronto, ON, Canada).

Vaccinia viruses

Recombinant Western Reserve VV F13L+, a wild-type virus with *lacZ* insertions,[49] and vvDD-R2R-Luc were used in this study. vvDD-R2R-Luc expresses an R2R segment, with a RFP insertion conjoined with Renilla luciferase via a foot-and-mouth disease virus 2A motif.[50] vvDD-R2R-Luc is derived from a double-deleted Western Reserve VV platform lacking TK and VGF.[8]

Creation of candidate VV deletion mutants

Wild-type Western Reserve VV $F13L^+$ was used as a backbone virus to generate the VV deletion mutants via homologous recombination. Using the primers listed in Table 2, segments of DNA (300–500 bp) flanking the left and right regions of wild-type N1L, K1L, K3L, A46R, or A52R VV genes were amplified by PCR. They were then inserted into a shuttle plasmid to flank an expression cassette consisting of an R2R segment and a xgprt gene under the regulation of the synthetic late pSyn/late promoter and the early/late p7.5 promoter, respectively (Figure 1). Monolayers of CV-1 cells at 80% confluence were infected with $F13L^+$ (MOI = 0.05) in DMEM-2.5% FBS for 2 h. Liposomal transfection (Lipofectamine 2000; Invitrogen, GIBCO) was then conducted as per the manufacturer's protocol using 2.5 μg of each individual shuttle plasmid DNA and 10 μL of liposome solution per well. Subsequent selection for xgprt expression from recombinant viruses in drugged DMEM (250 μg/mL xanthine, 14.9 μg/mL hypoxanthine, 25 μg/mL mycophenolic acid; Sigma Aldrich) was performed[51] for at least 5 rounds in CV-1 cells under an agarose overlay and confirmed for RFP expression. Final recombinant VV clones were expanded and DNA was extracted by Proteinase K digestion as previously described.[8] PCR confirmation was performed with the forward primer of the left flanking insert and the reverse primer of the right flanking insert of the corresponding viruses (Table 2).

Viral replication and spread in monolayers

Tumor cells were grown in 6-well plates overnight (5×10^5 cells/well for MC38; 1×10^6 cells/well for DLD-1 and A2780) and mock-treated or infected with candidate VVs or vvDD (MOI = 0.1) in 0.5 mL low-serum media (2.5% FBS) for 2 h. Plates were intermittently shaken during this time and then supplemented with complete media (10% FBS). To assess viral spread, we acquired bright-field and RFP images at 10× magnification using the Zeiss AxioObserver microscope (Carl Zeiss, Oberkochen, Germany) equipped with a Series 120Q Fluorescence Illumination unit (EXFO, Quebec City, Quebec, Canada). Images were taken with a Zyla 5.5 sCMOS camera (Andor Technologies, Belfast, UK). Percent area of RFP expression was quantified with Fiji ImageJ software. For viral replication assays, infected cells and supernatants were harvested using a Cell Scraper (Sarstedt, Germany), subjected to 3 freeze/thaw cycles, and sonicated. Viral load was quantified by plaque assay using CV-1 cells.

Viral cytotoxicity in monolayers

Tumor cells were grown in 96-well plates overnight (5×10^3 cells/well for MC38; 1×10^4 cells/well for DLD-1 and A2780) and mock-infected or infected with candidate VVs or vvDD (MOI = 1) in low-serum media (2.5% FBS) for 2 h and then supplemented with complete media (10% FBS). Viral cytotoxicity was evaluated using the MTS cell viability assay (CellTiter96 Aqueous One Solution, Promega, Madison, WI, USA) according to the manufacturer's protocol, with cell viability presented relative to mock-treated samples.

Tumor spheroid model

Spheroids were generated in 96-well round-bottomed plates coated with 1% polyHEMA (Sigma Aldrich) as previously described[29] and grown for 72 h. Spheroids were mock-infected or infected with candidate VVs or vvDD (MOI = 2) in DMEM-2.5% FBS for 2 h and then supplemented with DMEM-10% FBS. Bright-field and fluorescent confocal images were obtained with the LSM 700 Confocal Microscope (Carl Zeiss). Clonogenic assays were conducted at 96 hpi as previously described.[29] Surviving fraction was calculated as the number of colonies (>50 cells) divided by the number of cells originally seeded.

Mice

Female 6- to 8-week-old C57BL/6 and NU/NU athymic nude mice (Charles River Laboratories; Saint-Constant, QC, Canada) were used. All mice were housed under standard conditions and given food and water *ad lib*. Experimental protocols were approved by the Animal Care Centre, University Health Network, Toronto. Mice were euthanized when signs of morbidity including weight loss of >20%, a subcutaneous tumor >1.5 cm, extreme abdominal distention, difficulty breathing, moribund condition, or inability to obtain food or water, were present.

In vivo toxicity

Female C57BL/6 mice or NU/NU athymic nude mice (n = 6) were injected i.p. with the indicated doses of virus in Hank's balanced salt solution (HBSS; Invitrogen, GIBCO) or HBSS alone and monitored for signs of morbidity as above.

In vivo tumor models

Female C57BL/6 mice were injected i.p. with 10^5 MC38 cells in 2 mL serum-free media. Female NU/NU athymic nude mice were injected i.p. with 5×10^6 DLD-1 cells or 10^7 A2780 cells in 2 mL serum-free media. 12 days later, mice were injected i.p. with virus in 1 mL HBSS or control HBSS alone. Mice were followed for morbidity (n = 8) or sacrificed 6 days post-infection for biodistribution studies or immunohistochemistry (n = 3).

For biodistribution studies, tumor and non-tumor tissues were harvested into HBSS. Samples were homogenized with the TissueLyzer II (QIAGEN, Hilden, Germany), subjected to 3 freeze-thaw cycles, and sonicated prior to viral quantification by plaque assay with CV-1 cells. Titers were normalized to total protein per sample measured with the Pierce bicichoninic acid (BCA) protein assay kit (Thermo Fisher Scientific, Waltham, MA, USA). For immunohistochemistry, tumor tissues were fixed in 10% formalin for 48–72 h, transferred to 70% ethanol, and then embedded in paraffin. Tissue sections were stained with monoclonal rat anti-mouse F4/80 (cat # MCA497R, clone A3-1, dilution 1/2,000; Serotec/Bio-Rad, Hercules, CA, USA), CD3 (cat # A0452, clone F7.2.38 dilution 1/500; Dako, Santa Clara, CA, USA), B220 (cat #553084, clone RA3-6B2, dilution 1/2,000, BD PharMingen, San Jose, CA, USA), or monoclonal anti-mouse Ly6G (cat # 127601, clone 1A8, dilution 1/1,500; BioLegend, San Diego, CA, USA).

Statistical analysis

Data were analyzed by a two-tailed independent samples Student's t test between candidate VVs and vvDD where applicable. Survival curves were evaluated with the log-rank test. Graphs were generated with the Prism 5 Software (GraphPad Software, La Jolla, CA, USA). Values are presented as mean ± SEM (standard error of the mean) and p values < 0.05 were considered significant.

ACKNOWLEDGMENTS

This project was funded by the Lotte and John Hecht Foundation Innovation Grant of the Canadian Cancer Society Research Institute.

AUTHOR CONTRIBUTIONS

T.Y.H. was the primary researcher for all experiments and the primary author of the manuscript. J.A.M. was the senior researcher and author of the manuscript. D.F.S. was involved throughout the work and provided assistance with hypothesis development, experimental design, interpretation of findings, and manuscript editing. D.M. provided assistance with laboratory work and manuscript editing. L.O. provided laboratory technician support throughout the entirety of the research.

DECLARATION OF INTERESTS

The authors declare no competing interests.

REFERENCES

1. Ilkow, C.S., Swift, S.L., Bell, J.C., and Diallo, J.-S. (2014). From scourge to cure: tumour-selective viral pathogenesis as a new strategy against cancer. PLoS Pathog. *10*, e1003836.
2. Black, M.E., and Hruby, D.E. (1991). Structure and function of vaccinia virus thymidine kinase: Biomedical relevance and implications for antiviral drug design. Rev. Med. Virol. *1*, 235–245.
3. Buller, R.M., Smith, G.L., Cremer, K., Notkins, A.L., and Moss, B. (1985). Decreased virulence of recombinant vaccinia virus expression vectors is associated with a thymidine kinase-negative phenotype. Nature *317*, 813–815.
4. Stroobant, P., Rice, A.R., Gullick, W.J., Cheng, D.J., Kerr, M., and Waterfield, M.D. (1985). Purification and Characterization of Vaccinia Virus Growth Factor *42*, 383–393.
5. Perdiguero, B., and Esteban, M. (2009). The interferon system and vaccinia virus evasion mechanisms. J. Interferon Cytokine Res. *29*, 581–598.
6. Stojdl, D.F., Lichty, B.D., tenOever, B.R., Paterson, J.M., Power, A.T., Knowles, S., Marius, R., Reynard, J., Poliquin, L., Atkins, H., et al. (2003). VSV strains with defects in their ability to shutdown innate immunity are potent systemic anti-cancer agents. Cancer Cell *4*, 263–275.
7. Vander Heiden, M.G., Cantley, L.C., and Thompson, C.B. (2009). Understanding the Warburg Effect: The Metabolic Requirements of Cell Proliferation. Science *324*, 1029–1033.
8. McCart, J.A., Ward, J.M., Lee, J., Hu, Y., Alexander, H.R., Libutti, S.K., Moss, B., and Bartlett, D.L. (2001). Systemic cancer therapy with a tumor-selective vaccinia virus mutant lacking thymidine kinase and vaccinia growth factor genes. Cancer Res. *61*, 8751–8757.
9. Stojdl, D.F., Lichty, B., Knowles, S., Marius, R., Atkins, H., Sonenberg, N., and Bell, J.C. (2000). Exploiting tumor-specific defects in the interferon pathway with a previously unknown oncolytic virus. Nat. Med. *6*, 821–825.
10. Damon, I. (2013). Fields Virology. In Fields Virology, 6thed, Sixth Edition, D.M. Knipe and P.M. Howley, eds. (Philadelphia: Lippincott Williams & Wilkins), pp. 2161–2184.
11. Moss, B. (2013). Fields Virology. In Fields Virology, 6thed, D. Knipe and P. Howley, eds. (Philadelphia: Lippincott Williams & Wilkins), pp. 2130–2160.
12. McFadden, G. (2005). Poxvirus tropism. Nat. Rev. Microbiol. *3*, 201–213.
13. Belongia, E.A., and Naleway, A.L. (2003). Smallpox vaccine: the good, the bad, and the ugly. Clin. Med. Res. *1*, 87–92.
14. Lane, J.M., Ruben, F.L., Neff, J.M., and Millar, J.D. (1970). Complications of smallpox vaccination, 1968: results of ten statewide surveys. J. Infect. Dis. *122*, 303–309.
15. Heo, J., Reid, T., Ruo, L., Breitbach, C.J., Rose, S., Bloomston, M., Cho, M., Lim, H.Y., Chung, H.C., Kim, C.W., et al. (2013). Randomized dose-finding clinical trial of oncolytic immunotherapeutic vaccinia JX-594 in liver cancer. Nat. Med. *19*, 329–336.
16. Zeh, H.J., Downs-Canner, S., McCart, J.A., Guo, Z.S., Rao, U.N.M., Ramalingam, L., Thorne, S.H., Jones, H.L., Kalinski, P., Wieckowski, E., et al. (2015). First-in-man study of western reserve strain oncolytic vaccinia virus: safety, systemic spread, and antitumor activity. Mol. Ther. *23*, 202–214.
17. Kim, J.H., Oh, J.Y., Park, B.H., Lee, D.E., Kim, J.S., Park, H.E., Roh, M.S., Je, J.E., Yoon, J.H., Thorne, S.H., et al. (2006). Systemic armed oncolytic and immunologic therapy for cancer with JX-594, a targeted poxvirus expressing GM-CSF. Mol. Ther. *14*, 361–370.
18. Smith, G.L., Symons, J.A., Khanna, A., Vanderplasschen, A., and Alcamí, A. (1997). Vaccinia virus immune evasion. Immunol. Rev. *159*, 137–154.
19. Thorne, S.H., Hwang, T.H.H., O'Gorman, W.E., Bartlett, D.L., Sei, S., Kanji, F., Brown, C., Werier, J., Cho, J.H., Lee, D.E., et al. (2007). Rational strain selection and engineering creates a broad-spectrum, systemically effective oncolytic poxvirus, JX-963. J. Clin. Invest. *117*, 3350–3358.
20. Stack, J., Haga, I.R., Schröder, M., Bartlett, N.W., Maloney, G., Reading, P.C., Fitzgerald, K.A., Smith, G.L., and Bowie, A.G. (2005). Vaccinia virus protein A46R targets multiple Toll-like-interleukin-1 receptor adaptors and contributes to virulence. J. Exp. Med. *201*, 1007–1018.
21. Maloney, G., Schröder, M., and Bowie, A.G. (2005). Vaccinia virus protein A52R activates p38 mitogen-activated protein kinase and potentiates lipopolysaccharide-induced interleukin-10. J. Biol. Chem. *280*, 30838–30844.
22. Maluquer de Motes, C., Cooray, S., Ren, H., Almeida, G.M.F., McGourty, K., Bahar, M.W., Stuart, D.I., Grimes, J.M., Graham, S.C., and Smith, G.L. (2011). Inhibition of apoptosis and NF-κB activation by vaccinia protein N1 occur via distinct binding surfaces and make different contributions to virulence. PLoS Pathog. *7*, e1002430.
23. Bartlett, N., Symons, J.A., Tscharke, D.C., and Smith, G.L. (2002). The vaccinia virus N1L protein is an intracellular homodimer that promotes virulence. J. Gen. Virol. *83*, 1965–1976.
24. Liu, Z., Wang, S., Zhang, Q., Tian, M., Hou, J., Wang, R., Liu, C., Ji, X., Liu, Y., and Shao, Y. (2013). Deletion of C7L and K1L genes leads to significantly decreased virulence of recombinant vaccinia virus TianTan. PLoS ONE *8*, e68115.
25. Cruz, A.G.B., Han, A., Roy, E.J., Guzman, A.B., Miller, R.J., Driskell, E.A., O'Brien, W.D., and Shisler, J.L. (2017). Deletion of the K1L gene results in a vaccinia virus

that is less pathogenic due to muted innate immune responses, yet still elicits protective immunity. J Virol. *91*, e00542–17.

26. Langland, J.O., and Jacobs, B.L. (2002). The role of the PKR-inhibitory genes, E3L and K3L, in determining vaccinia virus host range. Virology *299*, 133–141.

27. Downs-Canner, S., Guo, Z.S., Ravindranathan, R., Breitbach, C.J., O'Malley, M.E., Jones, H.L., Moon, A., McCart, J.A., Shuai, Y., Zeh, H.J., and Bartlett, D.L. (2016). Phase 1 Study of Intravenous Oncolytic Poxvirus (vvDD) in Patients With Advanced Solid Cancers. Mol. Ther. *24*, 1492–1501.

28. Casagrande, N., Celegato, M., Borghese, C., Mongiat, M., Colombatti, A., and Aldinucci, D. (2014). Preclinical activity of the liposomal cisplatin lipoplatin in ovarian cancer. Clin. Cancer Res. *20*, 5496–5506.

29. Ottolino-Perry, K., Tang, N., Head, R., Ng, C., Arulanandam, R., Angarita, F.A., Acuna, S.A., Chen, Y., Bell, J., Dacosta, R.S., and McCart, J.A. (2014). Tumor vascularization is critical for oncolytic vaccinia virus treatment of peritoneal carcinomatosis. Int. J. Cancer *134*, 717–730.

30. Kirn, D.H., Wang, Y., Le Boeuf, F., Bell, J., and Thorne, S.H. (2007). Targeting of interferon-beta to produce a specific, multi-mechanistic oncolytic vaccinia virus. PLoS Med. *4*, e353.

31. Terawaki, S., Chikuma, S., Shibayama, S., Hayashi, T., Yoshida, T., Okazaki, T., and Honjo, T. (2011). IFN-α directly promotes programmed cell death-1 transcription and limits the duration of T cell-mediated immunity. J. Immunol. *186*, 2772–2779.

32. Christian, S.L., Zu, D., Licursi, M., Komatsu, Y., Pongnopparat, T., Codner, D.A., and Hirasawa, K. (2012). Suppression of IFN-induced transcription underlies IFN defects generated by activated Ras/MEK in human cancer cells. PLoS ONE *7*, e44267.

33. Hirschhaeuser, F., Menne, H., Dittfeld, C., West, J., Mueller-Klieser, W., and Kunz-Schughart, L.A. (2010). Multicellular tumor spheroids: an underestimated tool is catching up again. J. Biotechnol. *148*, 3–15.

34. Kaiser, W.J., and Offermann, M.K. (2005). Apoptosis induced by the toll-like receptor adaptor TRIF is dependent on its receptor interacting protein homotypic interaction motif. J. Immunol. *174*, 4942–4952.

35. Sakamoto, K., Maeda, S., Hikiba, Y., Nakagawa, H., Hayakawa, Y., Shibata, W., Yanai, A., Ogura, K., and Omata, M. (2009). Constitutive NF-kappaB activation in colorectal carcinoma plays a key role in angiogenesis, promoting tumor growth. Clin. Cancer Res. *15*, 2248–2258.

36. Konson, A., Mahajna, J.A., Danon, A., Rimon, G., and Agbaria, R. (2006). The involvement of nuclear factor-kappa B in cyclooxygenase-2 overexpression in murine colon cancer cells transduced with herpes simplex virus thymidine kinase gene. Cancer Gene Ther. *13*, 1093–1104.

37. Kelly, M.G., Alvero, A.B., Chen, R., Silasi, D.A., Abrahams, V.M., Chan, S., Visintin, I., Rutherford, T., and Mor, G. (2006). TLR-4 signaling promotes tumor growth and paclitaxel chemoresistance in ovarian cancer. Cancer Res. *66*, 3859–3868.

38. Cooray, S., Bahar, M.W., Abrescia, N.G.A., McVey, C.E., Bartlett, N.W., Chen, R.A.J., Stuart, D.I., Grimes, J.M., and Smith, G.L. (2007). Functional and structural studies of the vaccinia virus virulence factor N1 reveal a Bcl-2-like anti-apoptotic protein. J. Gen. Virol. *88*, 1656–1666.

39. Torres, A.A., Albarnaz, J.D., Bonjardim, C.A., and Smith, G.L. (2016). Multiple Bcl-2 family immunomodulators from vaccinia virus regulate MAPK/AP-1 activation. J. Gen. Virol. *97*, 2346–2351.

40. Pereira, A.C.T.C., Leite, F.G.G., Brasil, B.S.A.F., Soares-Martins, J.A.P., Torres, A.A., Pimenta, P.F.P., Souto-Padrón, T., Traktman, P., Ferreira, P.C.P., Kroon, E.G., and Bonjardim, C.A. (2012). A vaccinia virus-driven interplay between the MKK4/7-JNK1/2 pathway and cytoskeleton reorganization. J. Virol. *86*, 172–184.

41. Ottolino-Perry, K., Acuna, S.A., Angarita, F.A., Sellers, C., Zerhouni, S., Tang, N., and McCart, J.A. (2015). Oncolytic vaccinia virus synergizes with irinotecan in colorectal cancer. Mol. Oncol. *9*, 1539–1552.

42. Shen, Y., and Nemunaitis, J. (2005). Fighting cancer with vaccinia virus: teaching new tricks to an old dog. Mol. Ther. *11*, 180–195.

43. Naik, A.M., Chalikonda, S., McCart, J.A., Xu, H., Guo, Z.S., Langham, G., Gardner, D., Mocellin, S., Lokshin, A.E., Moss, B., et al. (2006). Intravenous and isolated limb perfusion delivery of wild type and a tumor-selective replicating mutant vaccinia virus in nonhuman primates. Hum. Gene Ther. *17*, 31–45.

44. Baranda-Avila, N., Mendoza-Rodríguez, C.A., Morimoto, S., Langley, E., and Cerbón, M. (2009). Molecular mechanism of cell proliferation in rodent uterus during the estrous cycle. J. Steroid Biochem. Mol. Biol. *113*, 259–268.

45. Kirn, D.H., and Thorne, S.H. (2009). Targeted and armed oncolytic poxviruses: a novel multi-mechanistic therapeutic class for cancer. Nat. Rev. Cancer *9*, 64–71.

46. Perdiguero, B., Gómez, C.E., Di Pilato, M., Sorzano, C.O.S., Delaloye, J., Roger, T., Calandra, T., Pantaleo, G., and Esteban, M. (2013). Deletion of the vaccinia virus gene A46R, encoding for an inhibitor of TLR signalling, is an effective approach to enhance the immunogenicity in mice of the HIV/AIDS vaccine candidate NYVAC-C. PLoS ONE *8*, e74831.

47. Di Pilato, M., Mejías-Pérez, E., Sorzano, C.O.S., and Esteban, M. (2017). Distinct Roles of Vaccinia Virus NF-κB Inhibitor Proteins A52, B15, and K7 in the Immune Response. J. Virol. *91*, e00575, e17.

48. John, L.B., Howland, L.J., Flynn, J.K., West, A.C., Devaud, C., Duong, C.P., Stewart, T.J., Westwood, J.A., Guo, Z.S., Bartlett, D.L., et al. (2012). Oncolytic virus and anti-4-1BB combination therapy elicits strong antitumor immunity against established cancer. Cancer Res. *72*, 1651–1660.

49. Roper, R.L., and Moss, B. (1999). Envelope formation is blocked by mutation of a sequence related to the HKD phospholipid metabolism motif in the vaccinia virus F13L protein. J. Virol. *73*, 1108–1117.

50. Lun, X.Q., Jang, J.H., Tang, N., Deng, H., Head, R., Bell, J.C., Stojdl, D.F., Nutt, C.L., Senger, D.L., Forsyth, P.A., and McCart, J.A. (2009). Efficacy of systemically administered oncolytic vaccinia virotherapy for malignant gliomas is enhanced by combination therapy with rapamycin or cyclophosphamide. Clin. Cancer Res. *15*, 2777–2788.

51. Earl, P., and Moss, B. (1998). Expression of Proteins in Mammalian Cells using Vaccinia Viral Vectors. In Current Protocols in Molecular Biology, F.M. Ausubel, R. Brent, R.E. Kingston, D.D. Moore, J.G. Seidman, J.A. Smith, and K. Struhl, eds. (New York: Greene Publishing Associates and Wiley Interscience), pp. 16.15.1–16.18.11.

52. DiPerna, G., Stack, J., Bowie, A.G., Boyd, A., Kotwal, G., Zhang, Z., Arvikar, S., Latz, E., Fitzgerald, K.A., and Marshall, W.L. (2004). Poxvirus protein N1L targets the I-kappaB kinase complex, inhibits signaling to NF-kappaB by the tumor necrosis factor superfamily of receptors, and inhibits NF-kappaB and IRF3 signaling by toll-like receptors. J. Biol. Chem. *279*, 36570–36578.

53. Shisler, J.L., and Jin, X.-L. (2004). The vaccinia virus K1L gene product inhibits host NF-kappaB activation by preventing IkappaBalpha degradation. J. Virol. *78*, 3553–3560.

54. Willis, K.L., Langland, J.O., and Shisler, J.L. (2011). Viral double-stranded RNAs from vaccinia virus early or intermediate gene transcripts possess PKR activating function, resulting in NF-kappaB activation, when the K1 protein is absent or mutated. J. Biol. Chem. *286*, 7765–7778.

55. Bravo Cruz, A.G., and Shisler, J.L. (2016). Vaccinia virus K1 ankyrin repeat protein inhibits NF-κB activation by preventing RelA acetylation. J. Gen. Virol. *97*, 2691–2702.

56. Meng, X., and Xiang, Y. (2006). Vaccinia virus K1L protein supports viral replication in human and rabbit cells through a cell-type-specific set of its ankyrin repeat residues that are distinct from its binding site for ACAP2. Virology *353*, 220–233.

57. Perkus, M.E., Goebel, S.J., Davis, S.W., Johnson, G.P., Limbach, K., Norton, E.K., and Paoletti, E. (1990). Vaccinia virus host range genes. Virology *179*, 276–286.

58. Carroll, K., Elroy-Stein, O., Moss, B., and Jagus, R. (1993). Recombinant vaccinia virus K3L gene product prevents activation of double-stranded RNA-dependent, initiation factor 2 alpha-specific protein kinase. J. Biol. Chem. *268*, 12837–12842.

59. Harte, M.T., Haga, I.R., Maloney, G., Gray, P., Reading, P.C., Bartlett, N.W., Smith, G.L., Bowie, A., and O'Neill, L.A.J. (2003). The poxvirus protein A52R targets Toll-like receptor signaling complexes to suppress host defense. J. Exp. Med. *197*, 343–351.